ELSEVIER

Thermochimica Acta 266 (1995) 31–47

thermochimica
acta

Obtaining further information from calorimetry ☆

G.P. Johari

Department of Materials Science and Engineering, McMaster University,
Hamilton, Ont. L8S 4L7, Canada

Abstract

This paper describes how calorimetry may be used to obtain two sets of information, namely, (i) the internal energy of a material's polymorphs by measuring their heat of solution as well as the effect of structural relaxation on this energy, and (ii) the amount of intergranular liquid (or a second solid phase) in polycrystalline solids. Experiments have confirmed the usefulness of the two methods, and have shown that a substantial amount of liquid at thermodynamic equilibrium is present at the grain junctions in a polycrystalline solid, or that such solids premelt significantly. The formalism and concepts developed here are expected to apply equally well to polycrystalline solids, which undergo order–disorder phase transformation, and where the more disordered phase remains at the grain junctions of the ordered phase.

Keywords: Calorimetry; Heat of solution; Internal energy; Polymorphism; Relaxation

---

1. Introduction

During his stay with us in 1984, Professor Suga had asked me if I thought there were further ways in which calorimetry could be used for understanding the behaviour of condensed matter. I had already used his and his coworkers' data to learn about the entropy contribution from localized configurational states in disordered solids [1] and about a problem with the thermodynamic continuity of the amorphous solid and supercooled liquid water [2]—this problem has since been resolved [3, 4]. So, at that time, I had no suitable reply. A decade of further experience has enabled me now to provide one. This article may henceforth be read as my tardy reply to Hiroshi Suga's query in 1984.

☆ Dedicated to Hiroshi Suga on the Occasion of his 65th Birthday.

SSDI 0040-6031(95)02341-0

Calorimetric studies provide, of course, a variety of information on a material's molecular behaviour and its overall state. To this I would like to add two more properties of considerable significance which may be measured by suitable calorimetric experiments. These are: (1) the internal energy of polymorphs of a material; and (2) the amount of intergranular liquid (or a more disordered solid phase) in polycrystalline solids. Theoretical aspects of these properties and of the methods to determine them are described in this article, and abbreviated results from studies intended to examine them are given. Such measurements may be extended to a variety of materials. This may help in achieving a further understanding of their behaviour.

2. The internal energy of a material's polymorphs

The current methods for determining the difference between the enthalpies H_{exc} or internal energies E_{exc} of two phases (polymorphs) of a material require measuring their C_p from near 0 K to the desired temperature T, and determining the difference between their respective integrals

$$H_{\text{exc}}(T) = \int_0^T (C_{p,2} - C_{p,1})\mathrm{d}T \tag{1}$$

if no phase transformation occurred in either phase on heating to T K. To determine the difference between the internal energies at 0 K, H°_{exc}, one requires further C_p data to a temperature T_x where both phases have transformed into a single phase, usually on melting congruently. In a general case of two polymorphs, 1 and 2, undergoing phase transformation, each at its characteristic temperature, T_1 and T_2, to the same third phase at a temperature T_x above T_2, H°_{exc} is given by

$$H^{\circ}_{\text{exc}} = \left(\int_0^{T_2} C_{p,2}\mathrm{d}T - \int_0^{T_1} C_{p,1}\mathrm{d}T\right) + \int_{T_1}^{T_2} C_{p,3}\mathrm{d}T + \Delta H_{t,1} - \Delta H_{t,2} \tag{2}$$

where the phase transformation temperature $T_2 > T_1$ and $\Delta H_{t,1}$ and $\Delta H_{t,2}$ are the heat of transformation of each phase to a third phase of heat capacity, $C_{p,3}$. For vitreous and crystalline phases

$$H^{\circ}_{\text{exc}} = \int_0^{T_x} C_{p,\text{vit}}\mathrm{d}T - \int_0^{T_\text{m}} C_{p,\text{crys}}\mathrm{d}T - \Delta H_\text{m} - \int_{T_\text{m}}^{T_x} C_{p,\text{liq}}\mathrm{d}T \tag{3}$$

The underlying principle of the above method is that when two phases of a material are brought from their different initial energy states to the same final energy state, the difference between the energy evolved (or absorbed) in doing so is equal to H_{exc}.

H_{exc} can also be determined by an alternative method in which two polymorphs of a material are dissolved in the same solvent at the same temperature. The difference between their heats of solution will be equal to the difference between the energies of their initial states at that temperature, because the final states of the two polymorphs dissolved in a given solvent are the same. Bianchi et al. [5] and Filisko [5] have indeed proposed this method for determining the difference between the structures of organic polymers. To elaborate this concept we consider the total energy change in the process in terms of the internal energy, instead of the enthalpy, because we use constant pressure, one atmospheric condition under which the pressure–volume $p\mathrm{d}V$ term is negligible.

In absolute terms, the difference between the enthalpies or energies of two polymorphs is written as

$$H_{\mathrm{exc}} = (E^{\circ} + \Sigma E^{i})_{\mathrm{phase\,1}} - (E^{\circ} + \Sigma E^{i})_{\mathrm{phase\,2}} \tag{4}$$

$$\Sigma E^{i} = E^{\mathrm{vib}} + E^{\mathrm{bond}} + E^{\mathrm{conf}} \tag{5}$$

where E° is the energy at 0 K (sum of the lattice and zero-point vibrational energies), and E^{i} is the internal energy associated with the ith feature at T above 0 K, i.e. E^{vib} for the vibrational, E^{bond} for the cohesive Van der Waals, covalent and hydrogen bond energy terms as the volume changes, and E^{conf} for the configurational contributions arising from rotameric or rotational transitions of molecular segments in the structure.

The heat of solution is written as

$$H^{\mathrm{s}} = (E^{\circ} + \Sigma E^{i})_{\mathrm{soln}} - [(E^{\circ} + \Sigma E^{i})_{\mathrm{solu}} + (E^{\circ} + \Sigma E^{i})_{\mathrm{solv}}] \tag{6}$$

where the subscript soln, solu and solv outside the brackets refer to the energy terms for solution, solute and solvent, respectively, and E° and ΣE^{i} are as defined for Eq. (4). The meaning of Eq. (6) is that the magnitude of H^{s} depends also upon the magnitude of $E^{\circ}_{\mathrm{soln}}$. If $E^{\circ}_{\mathrm{soln}}$ is large, H^{s} may be positive; if small it may be negative. When the solvent is the same for the dissolution of different phases at a given temperature, $(E^{\circ} + \Sigma E^{i})_{\mathrm{solv}}$ is the same for each case, as is $(E^{\circ} + \Sigma E^{i})_{\mathrm{soln}}$. Thus, these two terms cancel each other when Eq. (6) is used to obtain H_{exc}

$$H_{\mathrm{exc}} = -(H^{\mathrm{s}}_{1} - H^{\mathrm{s}}_{2}) \tag{7}$$

where H^{s}_{1} and H^{s}_{2} are the heats of solution of the two phases in a solvent at a fixed temperature. Thus the measurements of H^{s} will yield the enthalpy difference between different structures of a material. This is illustrated in Fig. 1.

Measurements of C_p against the temperature T of two phases yield the difference

$$\Sigma E^{i}_{1} - \Sigma E^{i}_{2} = \int_{0}^{T} C_{p,1}\mathrm{d}T - \int_{0}^{T} C_{p,2}\mathrm{d}T \tag{8}$$

where ΣE^{i} is defined by Eq. (5) and subscripts 1 and 2 refer to the two phases of a material. By combining Eqs. (4), (7) and (8) and rearranging

$$H_{\mathrm{exc}} = E^{\circ}_{1} - E^{\circ}_{2} + \int_{0}^{T} (C_{p,1} - C_{p,2})\mathrm{d}T \tag{9}$$

and on substituting Eq. (7) in (9)

$$E^{\circ}_{1} - E^{\circ}_{2} = -(H^{\mathrm{s}}_{1} - H^{\mathrm{s}}_{2}) - \int_{0}^{T} (C_{p,1} - C_{p,2})\mathrm{d}T \tag{10}$$

Thus the difference between the internal energies of two phases at 0 K can be determined from their heats of solution and the calorimetric enthalpy (known from the

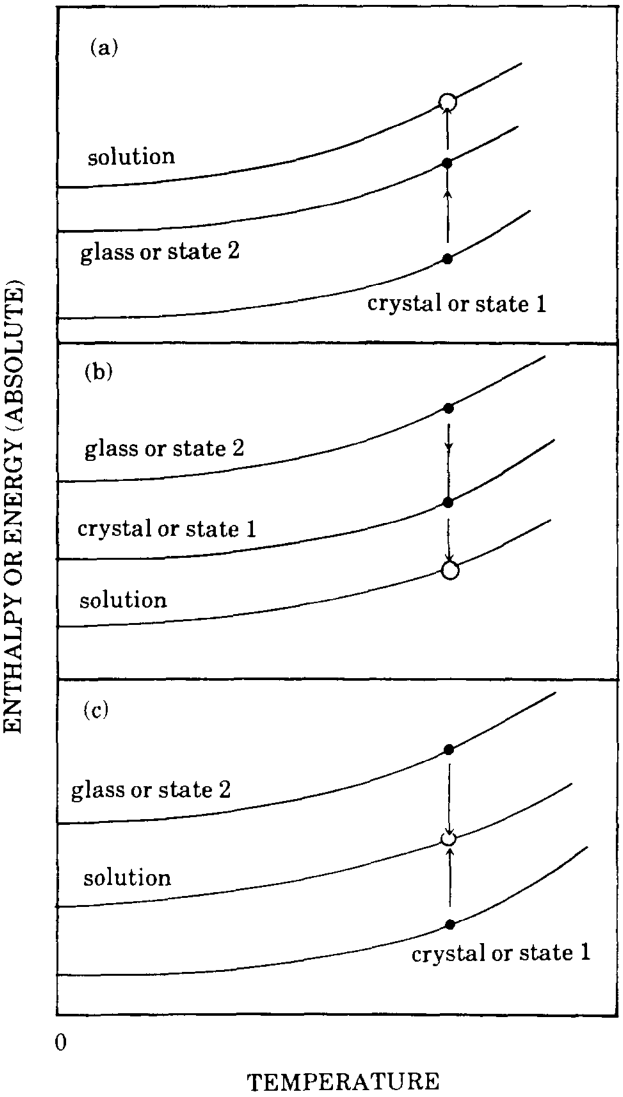

Fig. 1. The enthalpy of two states, 1 and 2, of a material and that of its solution. The curves illustrate (a) different amounts of heat absorbed and (b) different amounts of heat evolved on dissolution in a solvent. In (c), the curves show heat absorption when state 1 is dissolved and heat release when state 2 is dissolved. The effect illustrated in Fig. 1(c) has been observed for highly viscous glucose monohydrate and for glassy sucrose.

C_p measurements) at that temperature. It should be noted that the use of Eq. (7) for determining E°_{exc} requires no knowledge of the enthalpy of melting or of other phase transformations. Hence E°_{exc} of materials which melt incongruently, particularly many inorganic and most biological materials, may be determined by our procedure. This seems particularly valuable because E°_{exc} of such materials cannot be determined by the usual calorimetric methods.

To examine whether the procedure can be used successfully for materials, Salvetti et al. (in preparation) have measured the heats of solution of glassy and crystalline sucrose and viscous liquid and crystalline glucose monohydrate in pure water. They have found that heat is absorbed when crystalline sucrose dissolves in water and evolved when glassy sucrose does the same. This is an example of the case in Fig. 1(c). They also observed that more heat is absorbed when crystalline glucose monohydrate dissolves in water than released when its highly viscous liquid state dissolves in water, as is the case in Fig. 1(c).

I now consider the use of this method for studying the internal energy of amorphous solids, particularly glasses in their various states of structure. It is appropriate to recall that one of the characteristics of a glass is that its enthalpy decreases on spontaneous structural relaxation during its physical ageing, or as its fictive temperature T_f decreases spontaneously. (T_f is the temperature at which a metastable liquid in an internal equilibrium has the same energy as its glass.) As this occurs, E°_{exc} also decreases with T_f, so that the curve for H of glass plotted against temperature bodily moves closer to that of the crystal, but not by the same amount at all temperatures because both the vibrational contributions to the enthalpy of glass, and contributions from the availability of configurational states associated with its sub-T_g relaxations, also decrease, particularly when the glass densifies on ageing. This means that the exothermic H^S will decrease, or the endothermic H^S will increase on structural relaxation during the physical ageing of a glass. So, the heat of solution of a glass will be found to vary with its thermal history, as illustrated in Fig. 2, which corresponds to Fig. 1(c). This variation has now been observed in experiments on vitrified sucrose, thus confirming that the method proposed here can also be used for determining the thermal history and structural relaxation of vitrified solids. In my view, it may turn out to be an economic and more accurate alternative to the DSC and adiabatic calorimetry methods currently used for determining the change in the energy of a glass on its structural relaxation. The accuracy with which this change in energy can be determined depends upon the total heat of solution. If the latter is large in magnitude, relatively small differences between the heats of solution of two polymorphs may not be accurately determined. So, the accuracy of the method depends upon the position of the curve for solution relative to others in Figs. 1 and 2. The choice of solvent allows one to have some control over the magnitude of the heat of solution.

The heats of solution of inorganic and organic substances and metals have of course been widely studied for examining the validity of Raoult's and Henry's laws and for use in technology. Such data appear in tabulated form in handbooks of chemistry and physics. Drs. J.M. O'Reilly and I.M. Hodge, who read this manuscript, pointed out that a considerable amount of similar work has been done also for polymers not only for developing criteria for miscibility of polymer blends [6], but also for studying the swelling of polymers and the thermodynamics of polymer solutions in general [7–10]. In one particular study, they pointed out to me, the difference between the heat of solution of quenched atactic poly(methyl methacrylate) was measured in *o*-dichlorobenzene [10], and it was found that the heat of solution is more exothermic for the

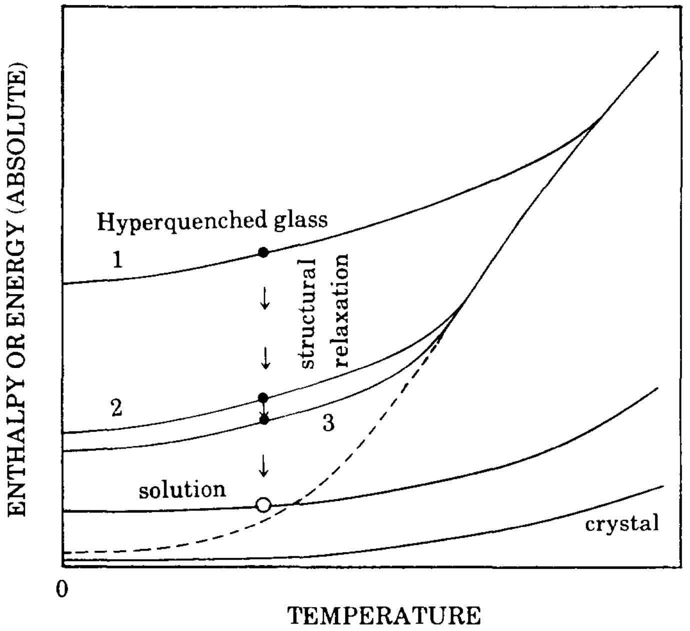

Fig. 2. The spontaneous decrease in the enthalpy of a glass on physical ageing, and its effect on the heat of solution. The illustration corresponds to conditions in Fig. 1(c). Conditions for Figs. 1(a) and 1(b) are not shown here. It should be noted that for conditions in Fig. 1(a), ageing will increase the heat absorbed and for 1(b), ageing will decrease the amount of heat released. Part of the effect illustrated in the figure has been observed for glassy sucrose.

quenched sample than for the as-reprecipitated sample at 313–328 K. This seems to be in accord with the illustration in Fig. 2. However, the authors [10] also observe that at 328 K and higher temperatures, the heats of solution of the quenched and as-reprecipitated samples became identical, which is not in accord with the illustration in Fig. 2. The authors [10] attributed this occurrence to crystallization of isotactic poly(methyl methacrylate) impurities whose T_g is $\sim$ 328 K. So, at least in a limited sense, one set of data on polymers does agree with our conclusion, implicit in Fig. 2, that a quenched sample will have a higher heat of solution than an annealed one.

3. Intergranular liquid in solids and the solid's extent of premelting

Most solids used commonly are polycrystalline, containing crystal grains of different sizes which form grain junctions where their boundaries meet. The requirements for a temperature-dependent new equilibrium between the interfacial free energy and enthalpy of melting causes the curved solid/liquid interface (boundary) to change in magnitude by melting or refreezing at the grain junctions. Hence, the liquid formed by the melting of crystal grains can remain at thermodynamic equilibrium with the solid, when confined to these grain junctions, even in the absence of any dissolved impurities, and so a small amount of (impurity-free) solid premelts, or melts below its usual thermodynamic melting point [11–14].

These grain junctions alter the physical properties of a solid and control the mass transfer of a liquid near its melting point. Materials produced by rapid solidification technology and by devitrification, as for example glassy water [3] and glassy metals, have grain sizes as low as 10 nm. Thus these solids contain a large population of grain junctions filled with crystal melt, as in ice, or a multicomponent melt of a different composition, as in devitrified metallic glasses and ceramics, which affects their electrical [15], mechanical and thermodynamic properties. The stability, and volume, of intergranular liquids in solids are, therefore, of considerable general interest. The thermodynamics of such solids can be written exactly in terms of the free energy changes that occur when grain junctions form, and this allows us to calculate the stability as well as the volume fraction of liquid phase present in a polycrystalline solid. This is done in the following, but before doing this we note that all concepts and formalism given hereafter apply equally well to substances undergoing solid–solid phase transformation with a change in entropy, i.e. first-order phase transitions. The high-temperature phase here is considered to be a liquid, but for solid–solid, order–disorder phase transformation, it would be the (more) disordered phase. All notations used here for the liquid will then refer to the high-temperature disordered solid phase. So, the formalism and discussion given here may be seen as generally valid when first-order phase transformations occur in polycrystalline solids.

3.1. Geometry and free energy of grain junctions

The geometry of two principal types of grain junctions is illustrated in Fig. 3, where (i) a curvilinear four-grain junction and (ii) the cross section of a vein formed by the meeting of three grains at 120° to one another are shown. A vein is considered to have a symmetrical cross section similar in shape to an equilateral curvilinear triangle. Both the volume of the pocket formed where four grains meet and the cross section of the vein are fixed by the dihedral angle 2θ. The volume of the pocket at the four-grain junction is given by

$$V_p = p_1 R_p^3 \tag{11a}$$

where p_1 is a dimensionless quantity related to the geometry of the pocket, as defined before [14], and $R_p = \sqrt{6}(h/\cos\theta)$ with h defined in Fig. 3 here and in Ref. [14].

The area of cross section or the volume per unit length of the vein formed at the three-grain junction is given by

$$A_v = c_1 R_v^2 \tag{11b}$$

where R_v is the radius of curvature of the sides of the vein and c_1 is a dimensionless quantity contained in square brackets in Eq. (2) in Ref. [14]. The volume of the liquid phase at thermodynamic equilibrium in relation to the grain structure, when no impurities are present, is determined by the relative surface energies of solid–solid and solid–liquid interfaces as well as by the temperature. This may be expressed in terms of

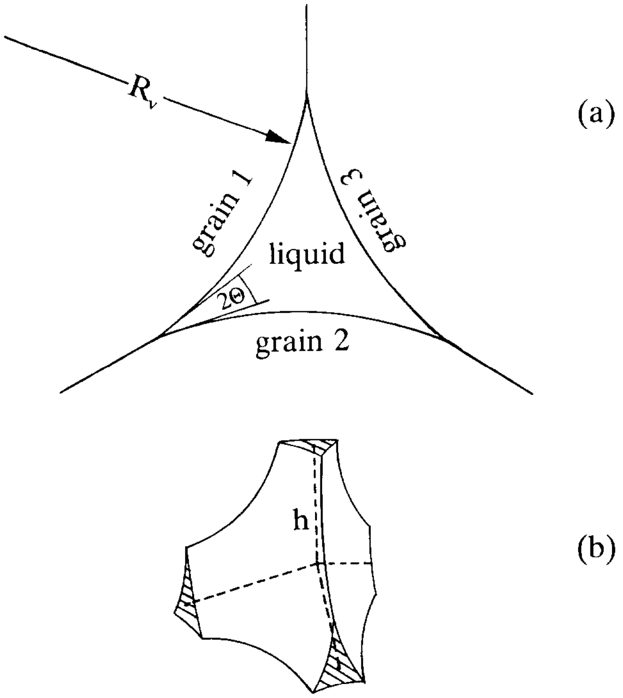

Fig. 3. (a) An illustration of the cross section of a vein filled with a liquid where three grains meet. Veins form at the expense of solid–solid grain boundaries. The figure is drawn for a dihedral angle of 25°. (b) An illustration of the four-grain junction forming a pocket from whose corners emerge the four veins; *h* refers to the distance as indicated.

free energy changes that occur when (i) solid melts to fill grain junctions, (ii) part of the grain–grain boundary vanishes, and (iii) grain–liquid interface forms at places where the grains meet and pockets of liquid form. For the formation of these pockets, the first of the above given three increases the free energy by

$$\Delta G_{\mathrm{sl,p}} = V_{\mathrm{p}} \Delta G_{\mathrm{m}} = p_1 \Delta G_{\mathrm{m}} R_{\mathrm{p}}^3 \tag{12}$$

where ΔG_{m} ($= \Delta T \Delta S_{\mathrm{m}}/V_{\mathrm{m}}$) is the free energy for melting, ΔS_{m} being the entropy of melting per mole, V_{m} the molar volume, and ΔT the undercooling below the melting point, T_{m}($\Delta T = T_{\mathrm{m}} - T$, where T is the temperature below T_{m}). The enthalpy of melting, $\Delta H_{\mathrm{m}} = T_{\mathrm{m}} \Delta S_{\mathrm{m}}$.

The disappearance of a part of the grain–grain boundary decreases the surface free energy by an amount

$$\Delta G_{\mathrm{gb,p}} = p_2 \Upsilon_{\mathrm{gb}} R_{\mathrm{p}}^2 \tag{13}$$

where Υ_{gb} is the grain boundary surface energy, and p_2 a dimensionless geometrical quantity [14].

The increase in the free energy at the solid–liquid interface at the pocket is given by

$$\Delta G_{\mathrm{int,p}} = p_3 \Upsilon_{\mathrm{int}} R_{\mathrm{p}}^2 \tag{14}$$

where $\Upsilon_{\mathrm{int}} (= \Upsilon_{\mathrm{gb}}/2\cos\theta)$ is the grain–liquid interfacial energy and p_3 is a dimensionless geometrical quantity [14].

The corresponding terms for the formation of veins where three grains meet are

$$\Delta G_{\mathrm{sl,v}} = A_{\mathrm{v}} \Delta G_{\mathrm{m}} = c_1 \Delta G_{\mathrm{m}} R_{\mathrm{v}}^2 \tag{15}$$

$$\Delta G_{\mathrm{gb,v}} = c_2 \Upsilon_{\mathrm{gb}} R_{\mathrm{v}} \tag{16}$$

and

$$\Delta G_{\mathrm{int,v}} = c_3 \Upsilon_{\mathrm{int}} R_{\mathrm{v}} \tag{17}$$

where c_1, c_2 and c_3 are the dimensionless quantities related to the geometry as defined before [14]. All free energies are for unit volume of the pockets and for volume per unit length of the veins, and it is assumed that Υ_{gb}, θ and ΔS_{m} do not vary with ΔT.

In the absence of impurities, the total change in the free energy on the formation of grain junctions is given by

$$\Delta G = \Delta G_{\mathrm{sl}} - \Delta G_{\mathrm{gb}} + \Delta G_{\mathrm{int}} \tag{18}$$

By eliminating the Υ_{gb} terms and differentiating Eq. (18) with respect to R, we obtain for conditions $(\partial G/\partial R) = 0$

$$R_{\mathrm{p,eq}} = 2\Upsilon_{\mathrm{int}}/\Delta G_{\mathrm{m}} = \frac{2\Upsilon_{\mathrm{int}} V_{\mathrm{m}}}{\Delta S_{\mathrm{m}} \Delta T} \tag{19}$$

for a pocket containing liquid at a four-grain junction.

Similarly for veins of water, we obtain

$$R_{\mathrm{v,eq}} = \frac{\Upsilon_{\mathrm{int}}}{\Delta G_{\mathrm{m}}} = \frac{\Upsilon_{\mathrm{int}} V_{\mathrm{m}}}{\Delta S_{\mathrm{m}} \Delta T} \tag{20}$$

The total volume of liquid contained in all grain junctions per unit volume of a solid or the volume fraction of the liquid at thermodynamic equilibrium at a given temperature and pressure is written as

$$V_l = N_{\mathrm{p}} V_{\mathrm{p}} + (l_{\mathrm{v}} - 4hN_{\mathrm{p}}) A_{\mathrm{v}} \tag{21}$$

where N_{p} is the number of pockets and l_{v} the total length of veins per unit volume of ice; V_{p} and A_{v} are defined by Eqs. (11a) and (11b), but with the radii of curvature referring to their equilibrium values, and h is the distance from the center of the curvilinear tetrahedral pocket to the plane of its truncation, as illustrated in Fig. 3(b)

$$h = \frac{R_{\mathrm{p}} \cos\theta}{\sqrt{6}} = \frac{2\Upsilon_{\mathrm{int}} V_{\mathrm{m}}}{\Delta S_{\mathrm{m}} \Delta T} \left(\frac{\cos\theta}{\sqrt{6}} \right) \tag{22}$$

For N_{g} number of uniform size or equiaxed grains per m^2 of a planar section, the grain size, $a = 1/\sqrt{N_{\mathrm{g}}}$ m. The total number of four-grain junctions or pockets per m^3 of the solid is given by [14]

$$N_p = \frac{4N_g}{a} \text{ or } N_p = \frac{4}{a^3} \tag{23}$$

The total length of randomly located veins in meters per m^3 of the solid, $l_v = 4N_g$, or $(4/a^2)$. By substituting for N_p, l_v and h in Eq. (21), the volume fraction of a liquid or the total volume of a liquid per unit volume of the solid becomes

$$V_l = v_l/(v_l + v_s) = 4(z_1 - z_2)(a\Delta T)^{-3} + 4z_3(a\Delta T)^{-2} \tag{24}$$

where $z_1 = 8\,p_1 e^3 \text{ m}^3 \text{ K}^3$, $z_2 = 8c_1 e^3 \cos\theta/\sqrt{6} \text{ m}^3 \text{ K}^3$, $z_3 = c_1 e^2 \text{ m}^2 \text{ K}^2$ and $e = \Upsilon_{int} V_m/\Delta S_m$; p_1 and c_1 are geometrical terms and e the thermodynamic term. Their definitions are given in Ref. [14]. The total volume of a liquid at the grain junction varies with temperature according to the magnitudes of the constants z_1, z_2 and z_3, which are a characteristic of a solid. For a given solid, it varies largely according to the inverse of ΔT^3 when $\Delta T \ll 1$ K and the inverse of ΔT^2 when $\Delta T \geq 1$ K.

According to Eq. (24), the total volume fraction of liquid in the pockets varies inversely with the cube of the grain size and in the veins with the square of the grain size at a constant temperature. For a given grain size, it varies inversely with the cube of ΔT for pockets and with the square of ΔT for veins. Note that the use of Eq. (24) for calculating the volume fraction is limited to certain conditions which require that the grain size be not less than twice the radius of curvature of the surfaces at the grain junctions. Since the radius of curvature of the surface is controlled by Υ_{int}, V_m, ΔS_m and ΔT (and grain size is not), this puts a lower limit for ΔT for a given solid. In general, no combination of grain size, Υ_{int}, V_m and ΔT should yield a volume fraction of liquid at grain junctions greater than 0.5 in an impurity-free polycrystalline solid at thermodynamic equilibrium.

The total free energy of an impurity-free polycrystalline mass in equilibrium at a certain temperature and pressure is the appropriately weighted sum of the ΔG_{sl}, ΔG_{gb} and ΔG_{int} terms. This weighting is with respect to the volume of all the pockets and veins in a polycrystalline solid, as described by Eqs. (19)–(22) in Ref. [14].

To illustrate the thermodynamics of polycrystalline solids, ice is used as an example. The total free energy of ice for grain size 0.1 mm was calculated from Eq. (18) and is plotted against the volume fraction of water at equilibrium in ice at 272.16 K ($\Delta T = 1$ K) and 272.66 K ($\Delta T = 0.5$ K) in Fig. 4. The two curves show a minimum at the equilibrium volume fraction of water which becomes deeper and moves to a larger volume fraction on increasing the temperature.

The effect of heating, and cooling, polycrystalline ice can now be expressed by drawing paths through the curves in Fig. 4. When ice kept at, say, 272.16 K ($\Delta T = 1$ K) is instantaneously heated to 272.66 K ($\Delta T = 0.5$ K), its free energy instantaneously decreases along a vertical path from point 1 to 2 on the curves corresponding to the two temperatures. The ice is no longer in its lowest free energy state and it melts at the grain junctions. Pockets of water grow in size and the veins dilate until the total volume of water corresponds to the new minimum denoted by 3 on the free energy curve. During this occurrence, ΔG_{sl}, ΔG_{gb} and ΔG_{int} will all decrease with increase in ΔT. Now, if the

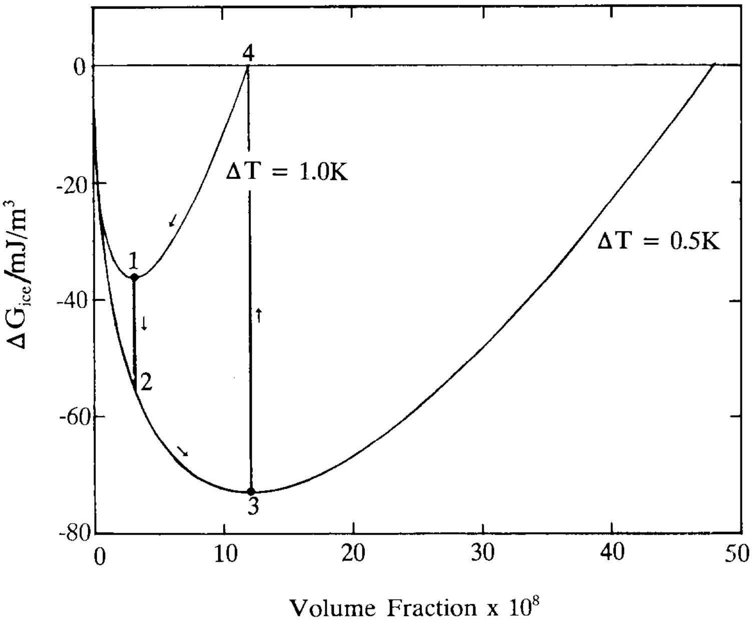

Fig. 4. The free energy change per m^3 of ice containing 0.1 mm size grains calculated for 272.16 and 272.66 K is plotted against the volume fraction of water in the ice. The path through the points 1 → 2 → 3 → 4 describes the melting and refreezing as discussed in the text.

ice is instantaneously cooled to 272.16 K, the total free energy instantaneously increases to point 4 and since ice is no longer in the lowest free energy state, a certain amount of water freezes, the veins and pockets contract, and the total volume of water will decrease to the equilibrium value denoted by 1. The path $1 \rightarrow 2 \rightarrow 3$ represents melting of ice at the grain junctions, and dilation of the water-containing pockets and veins; the path $3 \rightarrow 4 \rightarrow 1$ represents freezing of water at the grain boundaries and contraction of the water-containing pockets and veins. Since melting and freezing are almost instantaneous, a path connecting the free energy minima for different temperatures will describe the reversible change in the volume fraction of water on thermal cycling of ice. The thermodynamic path $1 \rightarrow 2 \rightarrow 3$ represents an absorption of heat without a temperature rise (as the latent heat for melting or ΔH_m), and the path $3 \rightarrow 4 \rightarrow 1$, a liberation of heat without a temperature decrease (as latent heat for crystallization, or $-\Delta H_m$). If ice initially contains dissolved impurities, the positions of the minima 1 and 2 will shift towards the right on each cycle as impurities become concentrated in water. Thus in an impurity-containing ice, the volume of water would increase with time. The observations of Fig. 4 are expected to be generally true for polycrystalline solids.

It is evident in Fig. 4 that a substantial amount of water exists in pure ice at thermodynamic equilibrium below its melting point, or that ice premelts. The amount changes mainly with the inverse square of the product of the grain size and undercooling according to Eq. (24) when its temperature reaches close to the melting point. The volume fraction of water for 1 mm grain size is 3.06×10^{-6} for $\Delta T = 0.01$. This volume of course increases when impurities are present.

The above-given calculations give theoretical basis to the conclusions obtained from the measured properties of microcrystalline solids. Dielectric measurements of microcrystalline cubic ice produced by devitrification of hyperquenched glassy water and vapour-deposited amorphous solid water had shown that microcrystalline cubic ice has a considerably high dielectric loss at temperatures 150–170 K which is attributed to the presence of water at grain junctions, and that this loss vanished when the grain growth was allowed to occur on thermal cycling to high temperatures but without transforming to hexagonal ice [15]. Such amounts of liquid in a fine grained solid at thermodynamic equilibrium will affect the compressibility, expansion coefficient and creep and fracture behaviours, particularly at temperatures when the liquid is not highly viscous or glassy.

When a polycrystalline solid premelts, it is expected that its measured heat capacity will be higher than that of its single crystal, for two reasons. (i) The heat capacity of the liquid contained at grain junctions is higher than that of the solid by an amount which is the sum of the contributions from the configurational degrees of freedom in the liquid and the differences between the low-frequency vibrational frequencies of the liquid and the crystal. This extra heat capacity is equal to the product of the C_p and the mole fraction of liquid per mole of the polycrystalline mass. (ii) The heat needed to melt the solid when the volume fraction of the liquid at equilibrium in its grain junctions increases on raising the temperature by 1 K. This is the latent heat, which does not raise the temperature. (This melting may be envisaged as an ideal heat sink.) Thus the total heat needed to raise the temperature of one mole of impurity-free polycrystalline solid by 1 K, or its measured C_p, is given by

$$C_{p,\mathrm{meas}} = X_\mathrm{s} C_{p,\mathrm{s}} + X_\mathrm{l} C_{p,\mathrm{l}} + \Delta H_\mathrm{m}(X_{\mathrm{l},(\Delta T - \delta T)} - X_{\mathrm{l},\Delta T})\delta T^{-1} \tag{25}$$

where X_s and X_l are mole fractions of the solid and liquid, respectively, in thermodynamic equilibrium at an average temperature of $(T_\mathrm{m} - \Delta T + 1/2\,\delta T)$. ΔT is the undercooling, and δT is the increase in the temperature observed during the C_p measurement after a known amount of heat is given to the solid sample. (Multiplication of the last term by δT^{-1} converts the quantity to per degree increase in temperature, as is required.) By substituting $(1 - X_\mathrm{l})$ for X_s and ΔC_p for $(C_{p,\mathrm{l}} - C_{p,\mathrm{s}})$, the excess measured C_p of polycrystalline solid over that of single crystal solid is given by

$$C_{p,\mathrm{exc}} = X_\mathrm{l}\Delta C_p + \Delta H_\mathrm{m}(X_{\mathrm{l},(\Delta\mathrm{T} - \delta T)} - X_{\mathrm{l},\Delta\mathrm{T}})\delta T^{-1} = (\Delta H_\mathrm{m}\Delta X_\mathrm{l})/\delta T \tag{26}$$

$X_\mathrm{l} = (v_\mathrm{l}\rho_\mathrm{l}/(v_\mathrm{s}\rho_\mathrm{s} + v_\mathrm{l}\rho_\mathrm{l}))$, where v and ρ are the volume and density, respectively. $X_\mathrm{l}\Delta C_p$ is usually less than 10^{-3}, so it may be neglected and X_l is the amount of liquid, calculated from Eq. (26).

From Eq. (26), it follows that $C_{p,\mathrm{exc}}$ will vanish when X_l and ΔX_l vanish and the measured C_p will be equal to the true C_p of the solid. Except for single crystal solids, $C_{p,\mathrm{exc}} > 0$, and for these the measured C_p is the sum of three terms, C_p of the crystal, C_p of the liquid, and the heat of melting divided by the temperature increase observed, all appropriately weighted by the mole fraction of the component. Amongst these, the last contribution, $(\Delta H_m \Delta X_l/\delta T)$ depends upon δT because ΔX_l increases nonlinearly with δT. To show this, I write Eq. (24) in the form

$$\Delta V_l = \frac{4(z_1 - z_2)}{a^3}\left[\frac{1}{(\Delta T + \delta T)^3} - \frac{1}{\Delta T^3}\right] + \frac{4z_3}{a^2}\left[\frac{1}{(\Delta T + \delta T)^2} - \frac{1}{\Delta T^2}\right] \tag{27}$$

In Eqs. (24) and (25), the term v_l is several orders of magnitude less than the term v_s. Hence, the magnitude of v_l (and v_w) in the denominators for the expressions for V_l, X_l (and X_w) may be neglected. Dividing X_l by V_l and taking the values at two temperatures to obtain ΔX_l and ΔV_l, yields

$$\Delta X_l \approx (\rho_l/\rho_s)\Delta V_l \tag{28}$$

To illustrate how ΔX_l varies with δT, I use the values of z_1, z_2 and z_3 for ice from Ref. [14], assume $a = 1$ μm, $\rho_{ice} = 0.93$ and $\rho_{water} = 1.0$ g ml^{-1}, and calculate ΔX_l for $\Delta T = 0.5, 0.6, 1$ and 2 K from Eqs. (26) and (27). This ΔX_l or ΔX_{water} is plotted against δT in Fig. 5. The progressively increasing slope of the plot with increase in δT and with decrease in ΔT clearly shows this non-linear dependence.

The increase in C_p observed in calorimetric measurements may be interpreted in two ways. Firstly in terms of the amount of heat consumed in melting ΔX_s amount of solid

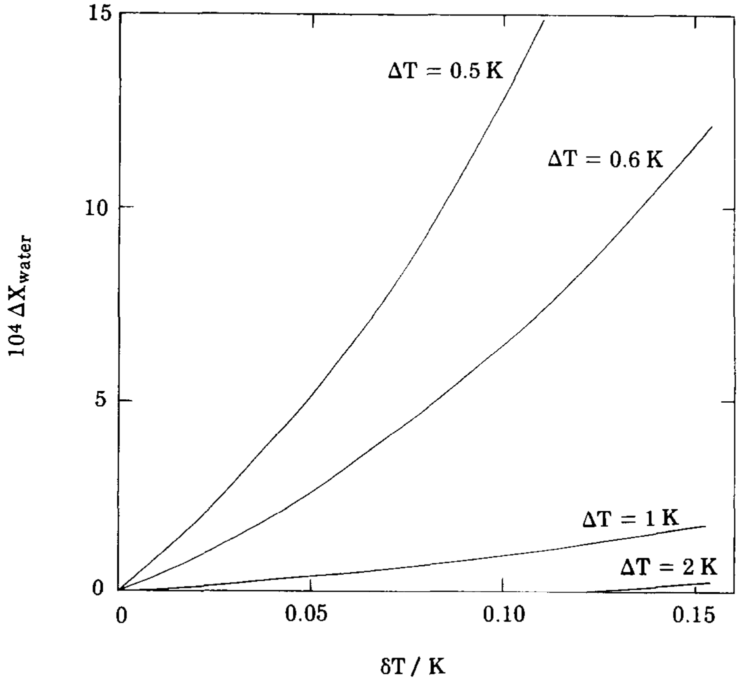

Fig. 5. The mole fraction of intergranular water in polycrystalline ice of grain size 1 μm is plotted against δT, the increase in temperature measured on heat input, as in the C_p measurement for different ΔT, the undercooling below the triple point of ice. The plot was calculated from Eqs. (27) and (28).

to ΔX_l amount of liquid without an increase in temperature—this is numerically equal to $\Delta H_m \Delta X_l$—and the remainder consumed in raising the sample's temperature which contains both the solid and intergranular liquid. Secondly, in terms of the amount of solid melted which predicts that for a fixed $C_{p,\mathrm{exc}}$ and δT, ΔX_l is high when ΔH_m is low, and for a fixed ΔX_l and δT, $C_{p,\mathrm{exc}}$ is high when ΔH_m is high. The validity of this statement and of the statement that the heat consumed in crystal melting is equal to $\Delta H_m \Delta X_l$, can be tested by further measurement of C_p of materials of the same grain size but different ΔH_m.

Both the heat consumed in premelting and ΔX_l may be determined when the amount of heat input and the observed rise in temperature, δT, of polycrystalline and large-crystal or single-crystal samples are known. For a polycrystalline sample, it yields the apparent C_p, for a single crystal the true C_p. This has been done for polycrystalline ice using different amounts of heat input.

Experiments by Salvetti et al [16] have shown that as much as 50% of the heat input is consumed in melting a small fraction of the solid at grain junctions in polycrystalline ice at $-0.6°C$, and the rest in raising the temperature of the sample. For example, in the measurement with heat input of 2.4 J to ~ 1 μm size grains containing polycrystalline ice at $-0.6°C$, the rise in temperature observed was 32.1 mK. This gave $C_{p,\mathrm{meas}} = 74.8$ J mol^{-1} K^{-1}. For large-crystal (or single-crystal) ice, $C_{p,\mathrm{meas}} = 40.6$ J mol^{-1} K^{-1}. Thus, $C_{p,\mathrm{exc}} = 34.2$ J mol^{-1} K^{-1} and from Eq. (26), $\Delta H_m \Delta X_{\mathrm{water}}$ is 1.1 J, which is 46% of the heat input used for the C_p measurement. Substituting 6.01 kJ mol^{-1} for ΔH_m, $\Delta X_{\mathrm{water}}$ formed on melting is 19.6×10^{-5}. When the heat input was 1.2 J, $\Delta X_{\mathrm{water}}$ was 7.3×10^{-5} and when it was 0.6 J, $\Delta X_{\mathrm{water}}$ was 3.25×10^{-5}. The experiments also demonstrated that $C_{p,\mathrm{meas}}$ or the apparent C_p of polycrystalline ice at $-0.6°C$ increased from 58.2 to 74.8 J mol^{-1} K^{-1} when the heat input used for the measurement was increased from 0.6 to 2.4 J. An abbreviated set of Salvetti et al.'s [16] C_p data for polycrystalline ice are shown in Fig. 6. These observations seem to confirm generally the conclusions of the formalism for premelting given in Ref. [14].

The amount of liquid at equilibrium with the solid or the extent of premelting may be determined from Eq. (24), provided the grain size, ΔH_m, the dihedral angle between the liquid and solid, and the interfacial (liquid–solid, and solid–solid) energies are known. (This calculation does not require C_p data.) But if the temperature rise, δT, on giving a certain amount of heat is known, as in the C_p measurements, ΔX_l can also be calculated from Eq. (27). For the theory to be valid, ΔX_l calculated from Eq. (27) should agree with that calculated from Eq. (26). This too has been examined by Salvetti et al.'s experiments [16]. From Eq. (27) and δT of 32.1 mK, 19.52 mK, and 10.3 mK, for heat input of 2.4, 1.2 and 0.6 J to polycrystalline ice assumed to contain uniform crystal grain size of 1 μm at $-0.6°C$, I calculated: $\Delta x_{\mathrm{water}} = 16.6 \times 10^{-5}$, 9.8×10^{-5} and 5.0×10^{-5}, respectively. The corresponding values calculated from $C_{p,\mathrm{exc}}$ data and Eq. (26) are: 19.6×10^{-5}, 7.3×10^{-5} and 3.25×10^{-5}. The first set of $\Delta X_{\mathrm{water}}$ differs from the second set by -18% to $+36\%$. The difference was less when the heat input used was large or δT was large. These discrepancies may arise partly from our assumption of a uniform grain size.

Salvetti et al. [16] also found that when ice was aged for 3.5 months at 248 K, its $C_{p,\mathrm{meas}}$ increased as the dissolved gaseous impurities in ice crystals diffused from the

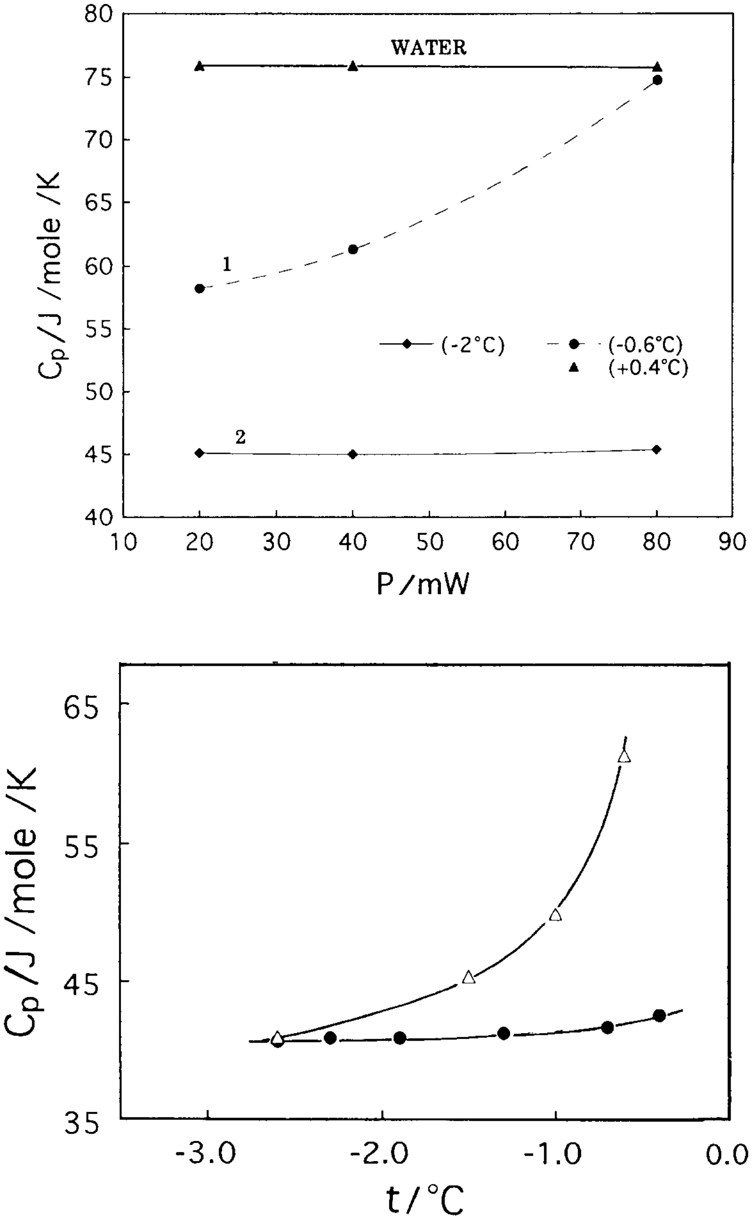

Fig. 6. (a) The measured C_p of microcrystalline ice (Δ) and large- or single-crystal ice (●) is plotted against the temperature of the sample. Data are taken from Ref. [16]. (b) The measured C_p of microcrystalline ice at −2° and −0.6°C and of water at +0.4°C is plotted against the power input in mW. The heat input is 30 times the power input. The data points are for 0.6, 1.2 and 2.4 J of heat input and are taken from Ref. [16].

grains into the intergranular water, lowered its triple point (and thereby decreased ΔT), and altered both the dihedral angle and the water–ice interfacial energy. In such a case, $C_{p,\text{meas}}$ is expected to reach ultimately a limiting value when the solubility equilibrium of impurities between the solid and liquid phases has been attained. This prediction is yet to be tested by an experiment.

Measurements of C_p of ordered polycrystalline solids below their order–disorder, solid–solid phase transformation temperatures are also needed in order to determine whether or not the above given concepts are experimentally verifiable, generally.

4. Concluding remarks

It is demonstrably clear that the two procedures for obtaining further information from calorimetry can be put into practice relatively easily, and the internal energy of a solid and the amount of liquid (or another solid present in the case of solid–solid phase transformation) present in polycrystalline solids be determined. Once the magnitude of the properties determined for several materials is confirmed by other measurements, e.g. internal energy from C_p measurements, and the amount of intergranular liquid (or a second solid phase) from energy diffraction measurements by suitable (but not yet available) methods, the technique proposed here can be used more efficiently and more economically than the other techniques.

I believe it would be useful to extend these studies to a wider class of materials and develop procedures for measuring accurately the heat of solution and C_p at temperatures close to the melting point of a solid. When more and accurate data become available, theoretical treatments of the zero-point internal energy of glass, to which attention is now being directed [17], and of the structure of intergranular liquid in solids may become possible.

Acknowledgements

This research was supported by a travel grant from the Association of Universities and Colleges in Canada and by the Natural Sciences and Engineering Research Council of Canada. I am also grateful to Drs. J.M. O'Reilly and I.M. Hodge for a constructive criticism of this work and particularly for bringing to my attention some of the work on polymers mentioned here.

References

[1] G.P. Johari, Annals N.Y. Acad. Sci., 279 (1976) 102; Phil. Mag., 41 (1980) 41.
[2] G.P. Johari, Phil. Mag., 35 (1977) 1077.
[3] G.P. Johari, A. Hallbrucker and E. Mayer, Nature, 330 (1987) 552.
[4] G.P. Johari, G. Fleissner, A. Hallbrucker and E. Mayer, J. Phys. Chem. 98 (1994) 4719.
[5] U. Bianchi, C. Cumberti, E. Pedemonte and C. Rossi, J. Polym. Sci., 7 (1969) 845, 855.
F. Filisko, Polym. Preprint, 15 (1974) 257.

[6] N.E. Weeks, F.E. Karasz and W.J. MacKnight, J. App. Phys., 48 (1977), 4068, and references therein.
[7] See a review by P.J. Flory, Disc. Faraday Soc., 49 (1970), 7.
[8] C.J.T. Landry and D.M. Teegarden, Macromol., 24 (1991) 4310, and references therein.
[9] F.E. Filisko and R.S. Raghava, J. Appl. Phys., 45 (1974) 4151.
[10] R.S. Raghava and F.E. Filisko, J. Appl. Phys., 45 (1974) 4155.
[11] F.C. Frank, Nature, 220 (1968) 350.
[12] J.F. Nye and F.C. Frank, in International Association of Scientific Hydrology Publication 95, (Symposium in Cambridge 1969, Hydrology of Glaciers), p. 157.
[13] R. Raj, Acta Metallurg., 38 (1990) 1413.
[14] G.P. Johari, W. Pascheto and S.J. Jones, J. Chem. Phys., 100 (1994) 4548; in Eq. (5) $\tan^2\theta$, should be read as $\sin^2\theta$.
[15] G.P. Johari, A. Hallbrucker and E. Mayer, J. Chem. Phys., 95 (1991) 2955; 97 (1992) 5851.
[16] G. Salvetti, E. Tombari and G.P. Johari, J. Chem. Phys., 102 (1995) 4987.
[17] G.P. Johari and J. Perez, Mol. Phys., 83 (1994) 235.